Turkish Journal of Electrical Engineering & Computer Sciences

http://journals.tubitak.gov.tr/elektrik/

Research Article

Turk J Elec Eng & Comp Sci
(2016) 24: 1325 – 1339
© TÜBİTAK
doi:10.3906/elk-1312-19

Power regulated DC/DC driver design by hierarchical control

Barış Baykant ALAGÖZ, Cemal KELEŞ, Asim KAYGUSUZ*, Yusuf KAPLAN, Abdulkerim KARABİBER

Department of Electrical and Electronics Engineering, Faculty of Engineering, İnönü University, Malatya, Turkey

Received: 03.12.2013 • **Accepted/Published Online:** 03.03.2014 • **Final Version:** 23.03.2016

Abstract: As a result of advances in solid-state power electronics, DC power distribution has found widespread usage due to its advantages. DC/DC converters, which are mainly used for voltage regulation, are fundamental components of DC power distribution systems. This paper presents a peak power controlled DC/DC converter design based on a two-layer hierarchical closed-loop control strategy for active DC power management. The proposed DC/DC converter design, called a power regulated DC/DC driver, limits output power according to current-voltage characteristic of a modified sigmoid function and it allows more secure and controllable power delivery in DC distribution buses. As a design example, we illustrate use of these DC/DC drivers in an active power distribution management application for electric vehicles. The MATLAB/Simulink simulation environment was used for the design and simulation of the proposed DC power distribution system. Simulation results indicate that the active power distribution management system composed of the power regulated DC/DC driver nodes can allow more reliable power distribution for electric vehicles.

Key words: DC/DC converters, hierarchical power system control, DC distribution, electric vehicles

1. Introduction

Modern electrical systems such as automation systems and consumer electronics need DC power. Due to advances in solid-state power electronics, implementation of power system components for more secure and smart DC distribution is possible today. Hence, DC distribution systems have begun to appear more frequently in daily life. Due to advantages of DC power distribution and DC energy storage systems, current trends indicate that DC power distribution will be preferred in the near future. Recently, DC power distribution has found applications in high-voltage electrical power transmission [1,2], residences [3–5], ships [6–8], and electric vehicles [9,10]. Future smart grid concepts contain DC power buses in microgrids to facilitate utilization of hybrid solar and wind energy systems [11,12].

DC distribution presents many advantages compared to AC power distribution [13]: 1) DC power is safe for human health as DC distribution systems do not cause strong electromagnetic oscillations and therefore they emit less electromagnetic radiation compared to AC distribution systems. 2) DC distribution systems also cause less electromagnetic interference because of the suppression of periodic oscillations. DC distribution can considerably enhance the electromagnetic compatibility [14]. Hence, it is more suitable for power line communication applications [15]. 3) DC distribution eliminates problems regarding reactive power and therefore power losses decrease and power transmission becomes more efficient and stable [16]. 4) DC buses facilitate

*Correspondence: asim.kaygusuz@inonu.edu.tr

renewable energy integration for microgrids [3–5,11,12]. Renewable energy systems such as photovoltaic and fuel cells generate DC electricity [3]. Although wind turbines yield AC power, integration of the power of several wind turbines is achieved by DC distribution [17]. 5) DC power distribution is more compatible with modern energy storage systems (batteries, fuel cells, super capacitors, etc.) [18].

The most fundamental components of DC distribution systems are DC/DC converters that provide conversion from a DC voltage level to another DC voltage level [19]. DC/DC converters in DC power distribution systems perform like transformers in AC distribution systems. In particular, DC/DC converters, which are designed for smart grid applications, should present superior voltage stability and controllability features. In the literature, several DC/DC converter designs were suggested. These include the buck type DC/DC converter [20,21], boost type DC/DC converter [22], flyback DC/DC converter [23], and so on. The flyback type of DC/DC converters contain transformers to adjust voltage level and they use rectifiers to give DC output voltage. However, solid-state buck [20,21] and boost [22] converters mainly use a switched mode technique, where output voltage is formed on a load capacitor via a power electronics switch. The switches are mostly controlled by pulse width modulation (PWM) for chopping of input voltage. In order to improve voltage stability of DC/DC converter, closed loop PID controllers or sliding mode controllers were used to control PWM [20].

In previous works, hierarchical control strategy was applied for the control of hybrid electrical energy systems containing multiple energy sources [24]. Mboup et al. showed that energy coming from different kinds of energy sources can be efficiently distributed to various load types by hierarchical control strategy [24]. Thus, efficient management of hybrid power systems can be possible [24,25].

In our study, we applied a hierarchical control strategy to obtain a smart DC/DC driver component, which provides peak output power control. For this purpose, a two-level hierarchical control architecture is employed: in the bottom layer, a closed-loop PI control system is used for output voltage stability of a buck type DC/DC switched mode converter. The PI control in this layer exhibits satisfactory voltage stability [20,21]. In the top layer, a modified sigmoid function in a positive feedback loop performs maximum (peak) output power limitation of the DC/DC converter. Thus, the PI-controlled bottom control layer is driven according to the limited power current-voltage characteristic of the modified sigmoid function characteristics [26] and it turns the buck type DC/DC converter [20] into a power regulated DC/DC driver. The power regulated DC/DC drivers can be used for active DC power management in DC distribution buses.

The proposed power regulated DC/DC driver allows online (instant) control of peak load power drawn from the DC distribution system. Thus, DC buses, constructed by proposed DC/DC driver nodes, allow distributed peak power management. This makes the DC distribution system more secure and controllable. As a design example, we develop a MATLAB/Simulink simulation of an electric vehicle active power distribution management system based on distributed control of power regulated DC/DC drivers. In this simulation example, we designed a DC bus that delivers the required power from the high-energy battery packs to electrical systems of the electric vehicle via the proposed DC/DC driver nodes. Simulation results reveal effective management of power injection from battery packs to electrical systems of the vehicle. We observed that the proposed power regulated DC/DC driver makes the DC distribution system more controllable and thus more reliable.

2. Methodology and design

2.1. Theoretical background for power regulated DC/DC driver

Figure 1a illustrates the basic equivalent circuit diagram of switched mode DC/DC converters [20,21,27,28]. The model of this circuit can be expressed as [20]:

$$\frac{dI_L}{dt} = \frac{1}{L}(AV_I - V_L), \tag{1}$$

$$\frac{dV_L}{dt} = \frac{I_L}{C} - \frac{V_L}{RC}, \tag{2}$$

where V_I and I_I are input voltage and input current of the converter, and V_L and I_L are output voltage and current of the circuit, respectively. Parameter A denotes the state of the switch, defined as {0,1}, and the value of A is determined by the PWM block. R, L, and C represent electrical elements: the resistor, inductor, and capacitor, respectively. The inductor (L) shows impedance for AC components and it is used to suppress harmonics. The capacitor (C) collects charges and establish output voltage (V_L) for the load resistance (R).

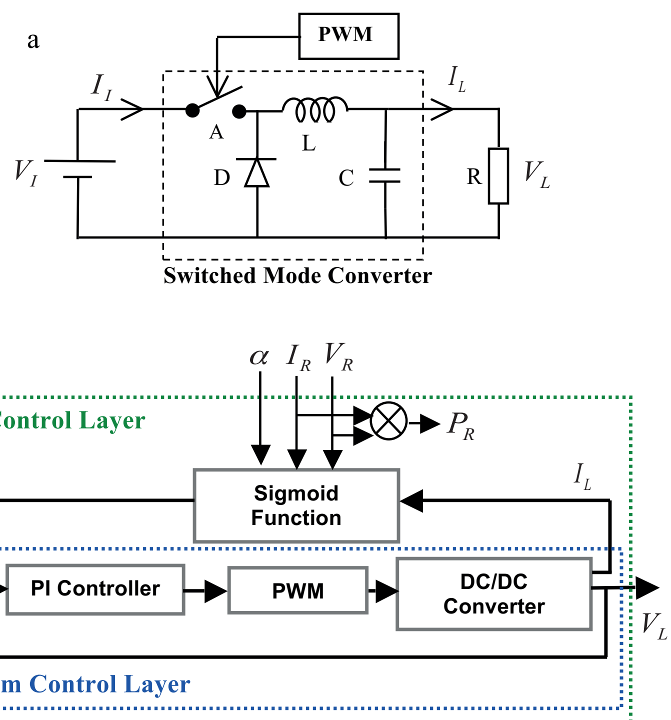

Figure 1. (a) Basic equivalent circuit diagram for switched mode DC/DC converter [20,21], (b) functional block diagram of two-layer hierarchical control architecture applied for power regulated DC/DC driver.

Figure 1b shows the functional block diagram of the two-layer hierarchical control architecture applied for the power regulated DC/DC driver. In the bottom layer, the switched mode circuit illustrated in Figure 1a is controlled by the closed-loop PI control structure. Voltage output of the power regulated DC/DC driver (V_L) provides negative feedback for the bottom layer control loop. This layer equalizes output voltage of the DC/DC driver to the reference voltage V provided by the top layer control structure. In the top control layer illustrated in Figure 1b, output current I_L provides a positive feedback for the reference input (V) via the modified sigmoid function. The modified sigmoid function implements a power limited voltage source characteristic [26]. The sigmoid function is commonly used in artificial neural networks for nonlinear output limiting. We employed a modified version of this function to obtain power limited current-voltage characteristics. The top layer controls the bottom layer for desired output voltage and desired power limitation.

In simulations, PI controller coefficients are configured to $k_p = 5$ and $k_i = 1$ in order to obtain satisfactory voltage stability by set and trial method. The PI control system leads to approximation of voltage error to zero, $\lim_{t\to\infty} e(t) = \lim_{t\to\infty}(V - V_L) = 0$, and thus stabilizes output voltage of the DC/DC driver. The output current feedback in top layer drives the reference input (V) of the bottom layer according to the power limited current-voltage characteristic expressed by the following modified sigmoid function:

$$V = F_g(I_L(t), V_R, I_R, \alpha) = \frac{V_R}{1 + e^{\alpha(I_L(t) - I_R)}}, \tag{3}$$

where parameter α adjusts the voltage transition slope of the F_g function. The voltage transition takes place when output power of the DC/DC driver exceeds a maximum power point P_R. The maximum power point can be approximately written as $P_R = I_R V_R$, where V_R is the desired output voltage of the DC/DC power driver and I_R sets the maximum current for the DC/DC driver. V_R and I_R determine the maximum power point of the modified sigmoid function, given by Eq. (3). When the output power, $P_L = I_L V_L$, exceeds the maximum power point P_R, the top control layer decreases the output voltage according to Eq. (3). Thus, the top layer keeps the power injection from the DC/DC driver to electrical loads lower than P_R and prevents excessive power from being drawn from the DC/DC driver. This feature considerably enhances controllability and security of DC power distribution.

Figure 2a shows the power limited current-voltage characteristic implemented by the modified sigmoid function $V = F_g(I_L(t), V_R, I_R, \alpha)$ for various values of α. As seen in the figure, the parameter α can be used to adjust the slope of the transition region, and this also tunes the sharpness of the maximum power point as shown Figure 2b. When the power exceeds P_R as a result of an increase in the load current I_L, the output voltage of the DC/DC driver reduces according to $V = F_g(I_L(t), V_R, I_R, \alpha)$, as illustrated in Figure 2a. The reduction of output voltage of the DC/DC driver gradually decreases the output current, and thus power injection to the load decreases. Low α value provides slower decrease of output voltage when the maximum power point is exceeded. If a fast decrease of power insertion from the driver is desired, higher α values should be set to the modified sigmoid function.

Operation modes of the designed power limited DC/DC driver are summarized in Table 1.

Table 1. Operation modes of proposed power limited DC/DC driver according to conditions of V_R and I_R.

Condition	Operation	Explanation
$V_R = 0 \vee I_R = 0$	Interrupt power insertion	Output voltage is zero ($V_L = 0$)
$(V_R \neq 0 \wedge I_R \neq 0) \wedge P_L < P_R$	Normal operation	Works as a DC/DC converter with stabilized output voltage
$(V_R \neq 0 \wedge I_R \neq 0) \wedge P_L > P_R$	Power regulating operation	Reduces output voltages to limit power insertion

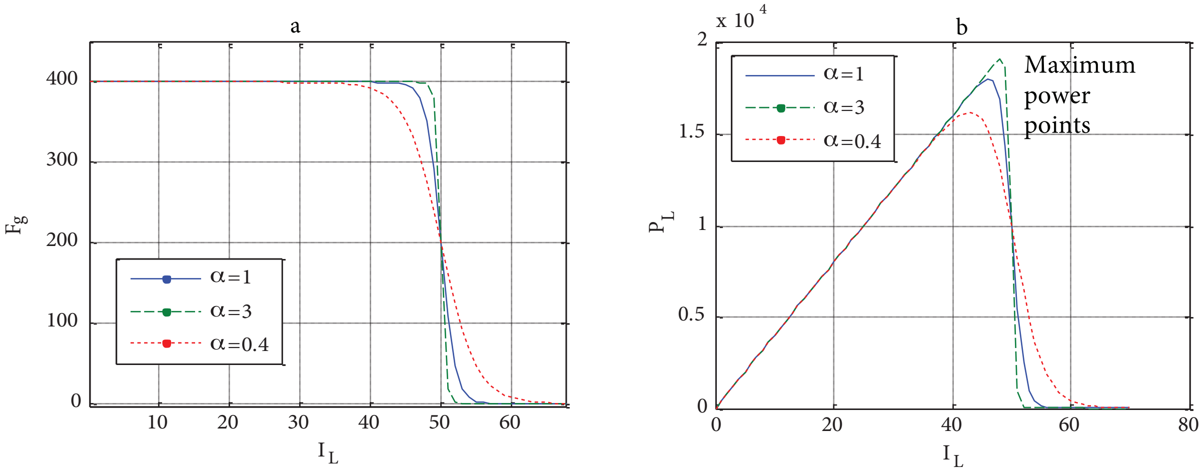

Figure 2. (a) Voltage-current characteristics obtained by modified sigmoid function $V = F_g(I_L(t), V_R, I_R, \alpha)$ for various α values, (b) the corresponding power-current characteristics showing peak power points.

2.2. Design and simulation of power regulated DC/DC driver

Figure 3a shows the MATLAB/Simulink design of the PI-controlled DC/DC converter block establishing the bottom control layer [20]. Figure 3b shows the MATLAB/Simulink design of the power regulated DC/DC driver, which is composed of bottom and top control layers. The top control layer includes the modified sigmoid function block for peak power limiting.

Figure 4 demonstrates simulation results of the conventional DC/DC converter with PI control (shown in Figure 3a) and the proposed power regulated DC/DC driver (shown in Figure 3b) for comparison proposes. In this simulation, $V_R = 400$ V and $I_R = 20$ A were configured and therefore the maximum power point of the DC/DC driver is obtained as about 8 kW. Since the load current increased to levels of 45 A at the 3rd second, power drawn by the load reached the level of 18 kW. In this condition, the conventional DC/DC converter continues 18 kW power injections to the load as seen in Figure 4. However, exceeding the maximum of power 8 kW, the power regulated DC/DC driver decreases the output voltage slowly until the load current comes below the reference current $I_R = 20$ A. The total power injection from the driver decreases to 3.6 kW and this protects the system against an excessive power insertion. While the power regulated DC/DC driver works in normal operation mode (see Table 1), if the load power reaches an undesired level, the driver goes into power regulating operation mode and it reduces output voltage to limit output power. This avoids long-term high power drawing from the system and makes the power management more secure.

3. An example application: a DC power distribution management for electric vehicles

This section demonstrates an example design for DC power distribution management of electric vehicles. This system is developed by using the proposed power regulated DC/DC driver nodes spreading over to the DC bus of the electric vehicle. Figure 5 shows a schematic diagram of the electric vehicle DC power distribution system. Current and voltage requirements of the vehicle components are estimated by help of electric vehicle design specifications reported in [29]. Power requirements are assumed for a small vehicle for urban transport.

The battery pack is assumed to provide 300 V output voltage as a result of serial connection of battery units. The output of the battery pack is connected to a 60 V DC bus via a power regulated DC/DC driver.

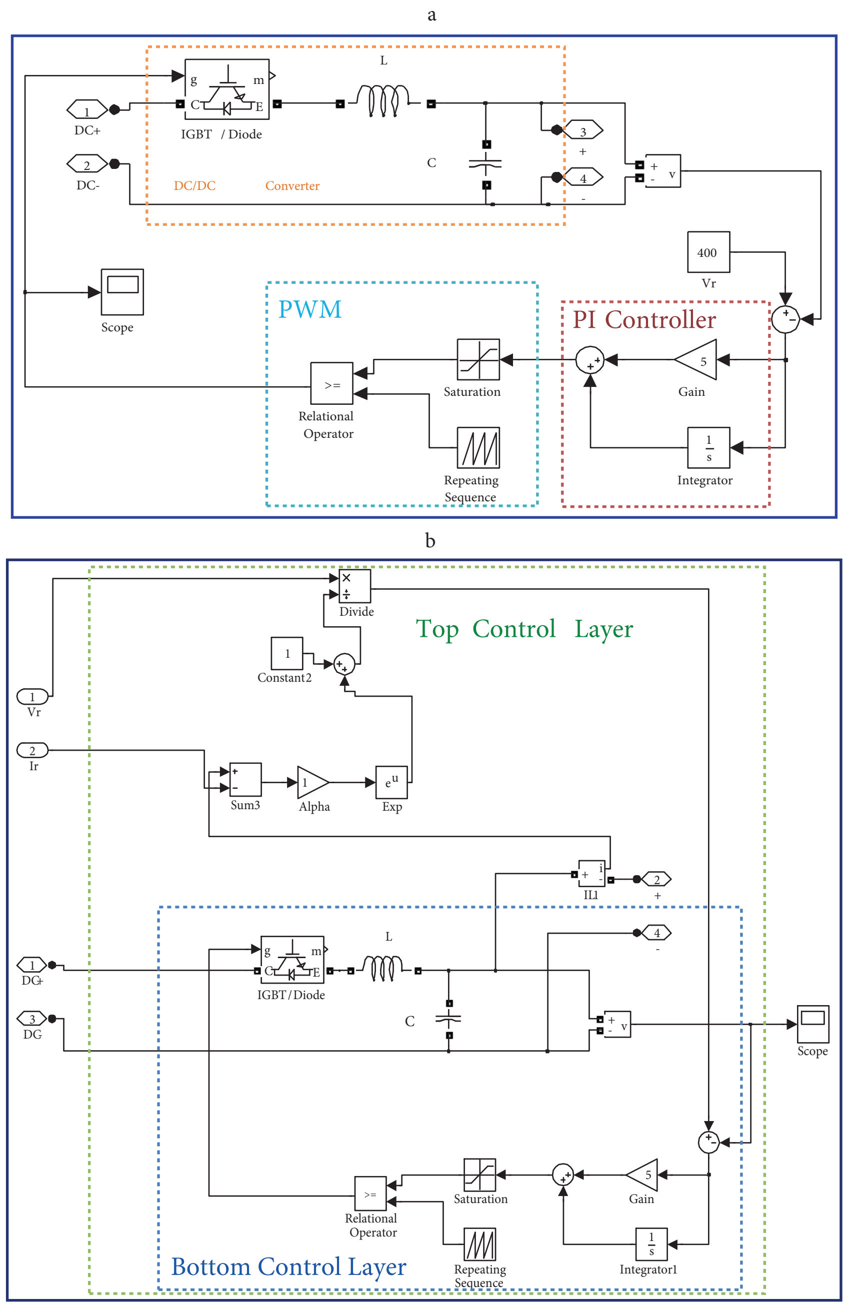

Figure 3. (a) MATLAB/Simulink design of PI-controlled DC/DC converter block ($k_p = 5$, $k_i = 1$, L $= 20.10^{-3}$ H, C $= 0.5$ F), (b) MATLAB/Simulink design of power regulated DC/DC driver ($k_p = 5$, $k_i = 1$, $\alpha = 1$).

This central DC/DC driver isolates the battery from the DC bus and it provides voltage stability of the DC bus under fluctuating demands of electrical subsystems. Electrical subsystems and components of the electric vehicle are connected to the 60 V DC distribution bus by peripheral DC/DC driver nodes. All DC/DC drivers are configured to L $= 20.10^{-3}$ H and C $= 0.5$ F to obtain a satisfactory DC voltage stability at the output. These nodes provide conversion of bus voltage to input voltage levels of electrical components, and thus more stable voltage and controllable power insertion from the bus to components can be achieved. Moreover, online management of power insertion from the battery to the DC bus and from the DC bus to electrical components can be possible by this distributed control strategy because every power regulated DC/DC driver node makes the system parts more observable and controllable.

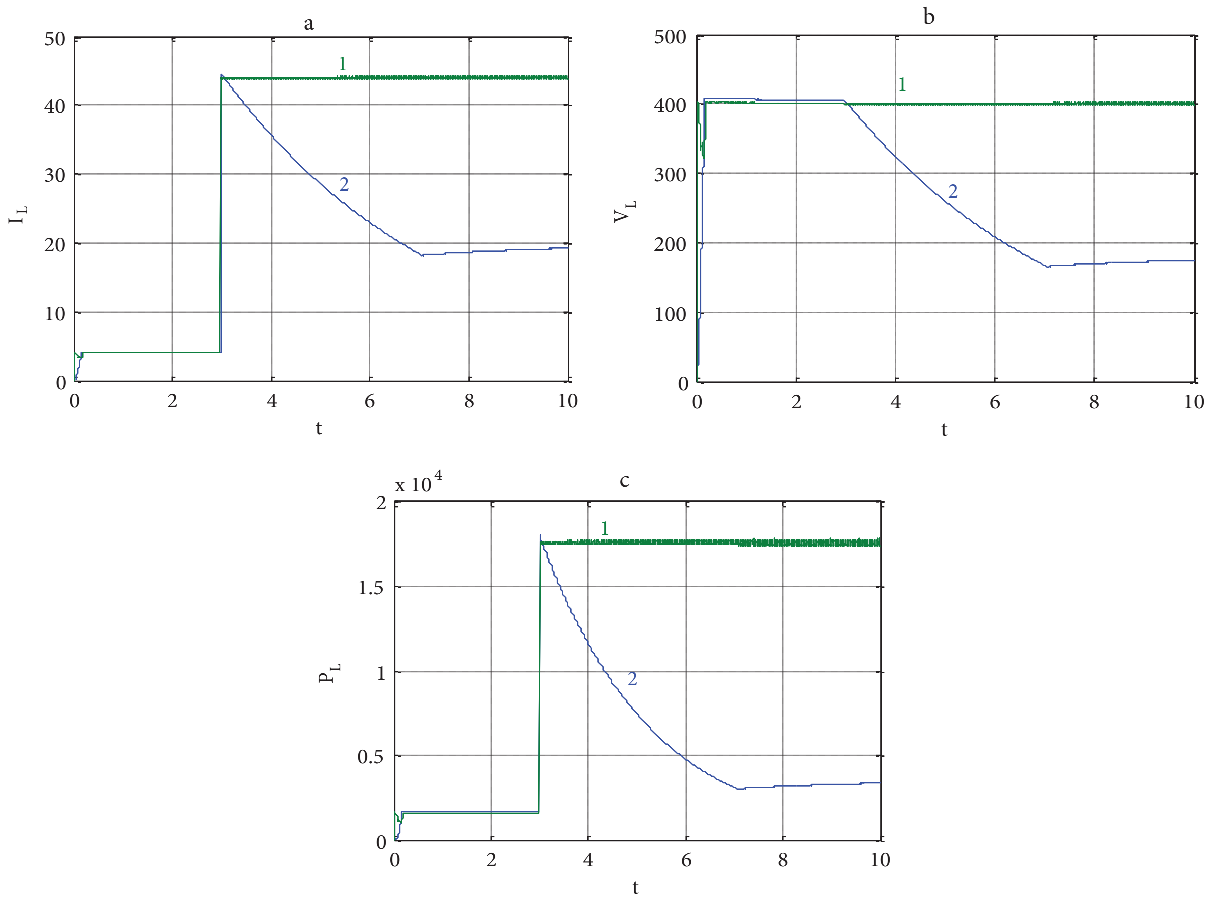

Figure 4. Simulation results obtained for DC/DC converter (label 1) and power regulated DC/DC driver (label 2).

Although low DC bus voltage (60 V) requires using thicker cables in cross-sections in distribution due to the requirement of high current flowing, a low-voltage DC bus is more secure and appropriate for electric vehicles. This is because high-voltage distribution bus becomes a serious risk factor for passenger and car electronics. We designed a 60 V DC distribution bus and assumed a maximum total current drawing of 220 A from the battery pack for full power operation of the electric vehicle.

Active power management by power regulated DC/DC driver nodes can offer the following advantages:

1) Active battery power management depending on power demands of system components: Power demand of electric vehicles varies depending on operation status. For instance, while parking, electric vehicles demand very low power only for security systems. While cruising, power demands of cars increase sharply depending on driving conditions. The power drawn from the battery should be actively managed depending on the operation status of electric vehicle. The active power management by the DC/DC driver enables the use of battery power more efficiently. In the case of electrical faults, it avoids high power being drawn from the battery pack and damage of battery cells.

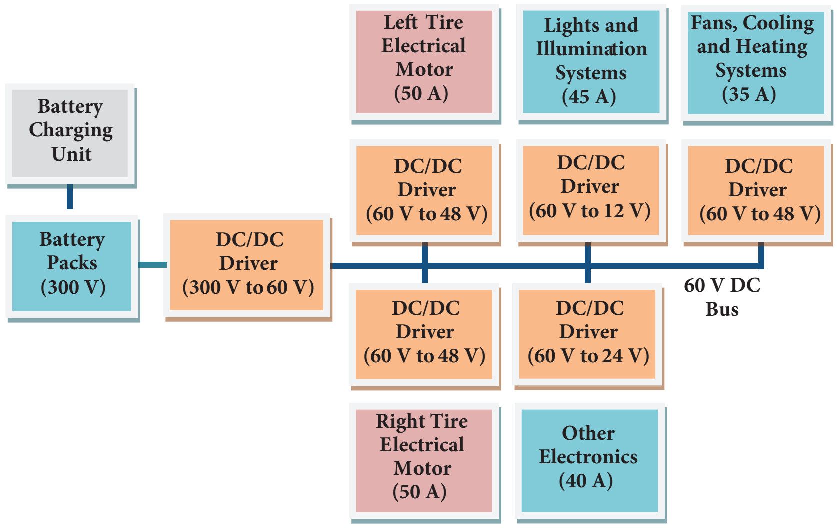

Figure 5. A schematic diagram of the electric vehicle DC power distribution system.

2) Battery protection and increasing the lifetime of battery units: The electric vehicle applications exhibit high power demands and long-term high current drawing from the battery packs. This leads to overheating and hence damages the battery cells. To prolong battery lifetime, power injection from the battery pack should be adjusted to avoid overheating. This is why there is a need for active power management to adjust power insertion of the battery pack according to the battery heat.

The power regulated DC/DC driver node between the DC distribution bus and battery pack supports modular battery management of the battery system. Multibattery systems use battery balancer units to improve battery efficiency and lifetime. In practice, modular battery management systems monitor battery parameters such as battery current, heat, and charges [30]. These battery parameters support the active power management system to regulate power injection from battery to system at healthy levels.

3.1. Active power management simulation

This section illustrates simulation of DC power management when the car begins to move at a constant speed. Table 2 describes electrical parameters of DC/DC drives (I_R, V_R, maximum power point P_R) used in the simulation of the electric vehicle.

Table 2. Electrical parameter setting of DC/DC drivers used in fault simulation.

DC/DC driver	Operation-status	Reference current (I_R)	Reference voltage (V_R)	Maximum power point (P_R)
60 V DC bus	Active - normal	220 A	60 V	13.2 kW
Left tire motor system	Active- normal	50 A	48 V	2.4 kW
Right tire motor system	Active - normal	50 A	48 V	2.4 kW
Lights and illumination systems	Active - normal	45 A	12 V	0.5 kW
Other electronics	Active - normal	40 A	24 V	0.9 kW
Fans, cooling and heating systems	Active - normal	35 A	48 V	1.6 kW

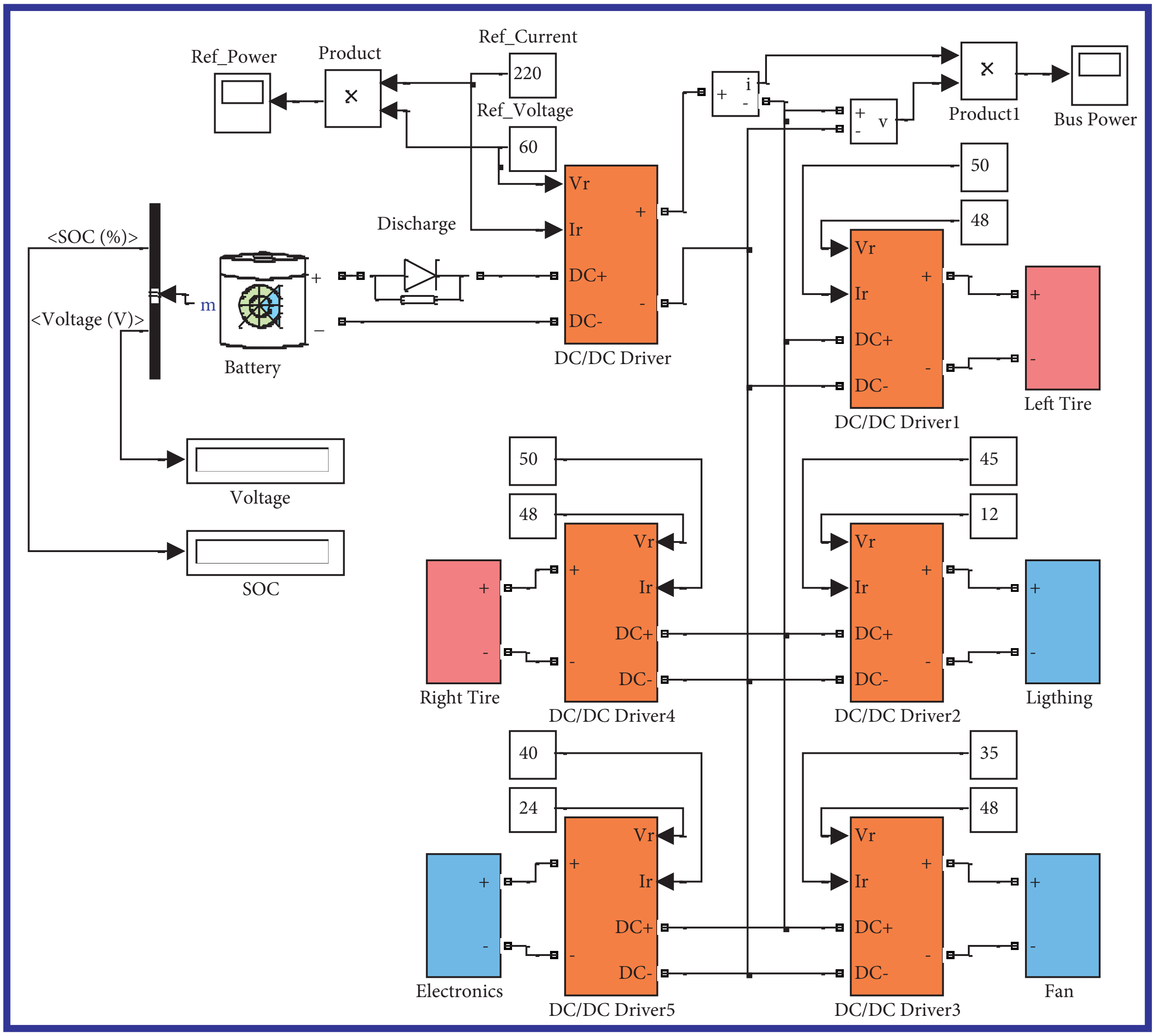

Figure 6. MATLAB/Simulink design of the electric vehicle DC power distribution system illustrated in Figure 5.

Figure 7 shows simulation results obtained from the output of the DC/DC driver of the left tire motor system. As seen in the figure, voltage, current, and power levels are well stabilized by the PI controller in the 0.5 s transient regime.

Figure 8 shows simulation results obtained from the output of the central DC/DC driver node located between the battery pack and 60 V DC bus. When the simulation is started, the electrical systems draw high current from the battery pack due to the startup transient regime of the systems. After voltage of the DC bus reaches stability at the level of 60 V, the system works in the steady-state regime until the end of simulation. The power system still allows instant high current and power drawings from the battery. The response of the active power system for a long-term high current being drawn from the battery is discussed in the following section.

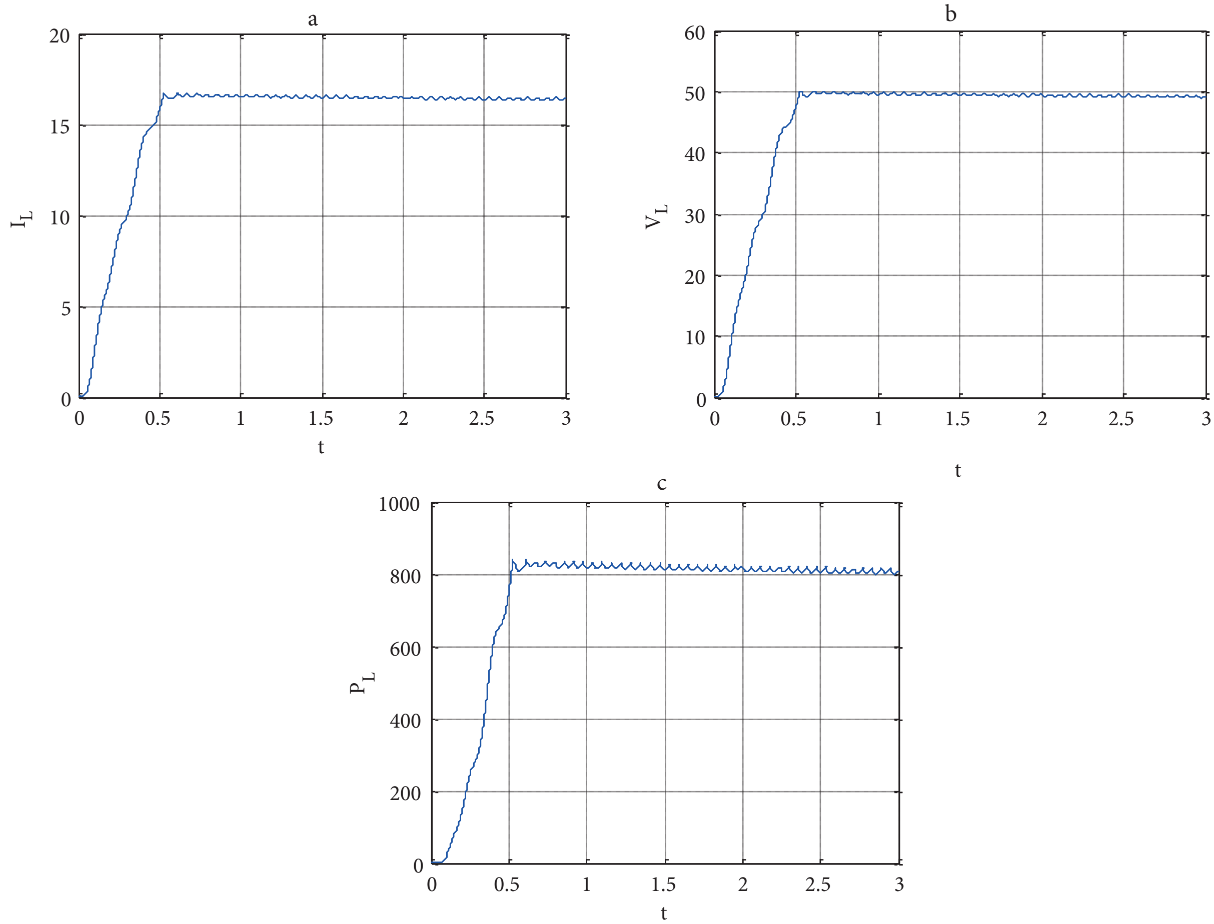

Figure 7. Simulation results obtained from power regulated DC/DC driver output of the left tire motor system.

3.2. Simulation for excessive power drawing fault

This section illustrates simulation results for a fault scenario causing excessive current drawing from the power system due to isolation corruption. The electrical parameters of DC/DC drives given in Table 2 are used in this scenario for normal operation of the electric vehicle.

In this simulation scenario, the left tire motor causes an electrical fault at the 2nd second and begins to draw excessive power from the DC bus. In these fault conditions, the simulation results demonstrate the response of the power distribution system. Isolation fault in the left tire motor system causes a long-term excess of 2.5 kW maximum power point limits of the DC/DC driver, and the DC/DC driver of the left tire motor decreases its power insertion to secure levels for the DC power system. This response prevents negative effects of this fault on operation of the DC bus and other systems. This gives us an opportunity to enforce faulty tire motor work in normal power ranges until secure stopping of the car without negatively affecting the operation of other system components. This asset is very essential to enhance the reliability of electric vehicle systems.

Figure 9 shows simulation results obtained from power regulated DC/DC driver outputs for the right tire motor system (label 1) and the left tire motor system (label 2). Due to persistent high current drawing of the faulty left tire motor system, the DC/DC driver decreases output voltage until the current reduces below the reference current of 50 A (see Table 2). This response of the DC/DC driver decreases power insertion for the

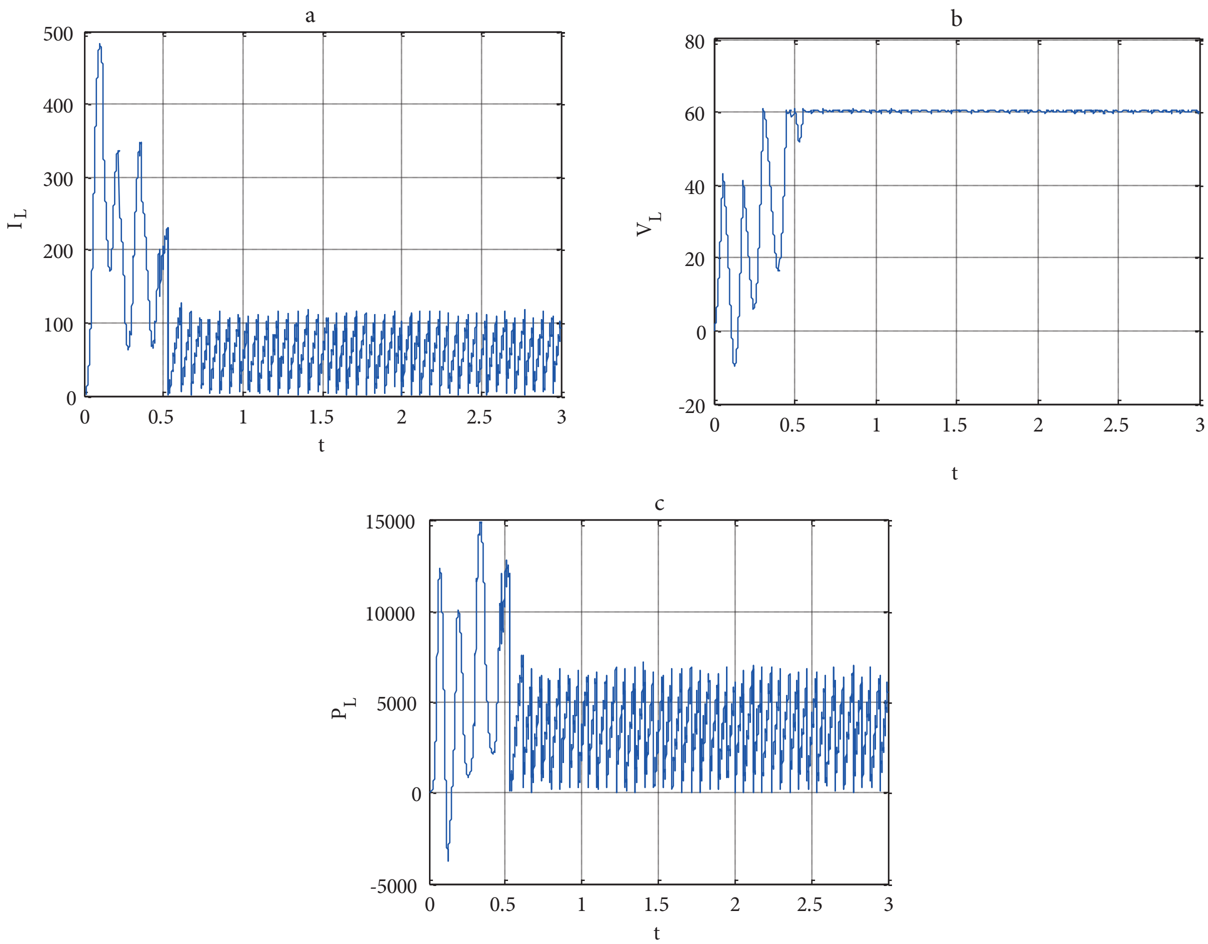

Figure 8. Simulation results obtained from the output of the central power regulated DC/DC driver supplying the 60 V DC bus.

faulty left tire in allowable ranges ($0 < P_L < P_R$) and enables it to work without influencing other systems.

Figure 10 shows electrical parameters of the 60 V DC bus. Three characteristic regions are seen in the figure. The first region, labeled by the mark 1, is the startup transient regime. The second region, labeled by the mark 2, is the steady-state region of normal operation, and the third region, labeled with the mark 3, illustrates working under fault conditions of the left tire motor. As seen from the figure, the fault causing high current and power drawings does not seriously affect DC bus voltage stability, and the power injection from the battery does not reach undesirably high rates for a long period. Other components of the electric vehicle can work normally under these heavy fault conditions and this can considerably enhance reliability of the power system.

4. Conclusions

Smart energy delivery is one of the most prominent subjects of the last decades. DC power distribution exhibits numerous advantages compared to AC distribution system. The modern DC power distribution systems should be designed to be controllable and observable by smart components. This study demonstrates design and utilization of a power regulated DC/DC driver component to build more secure and controllable power

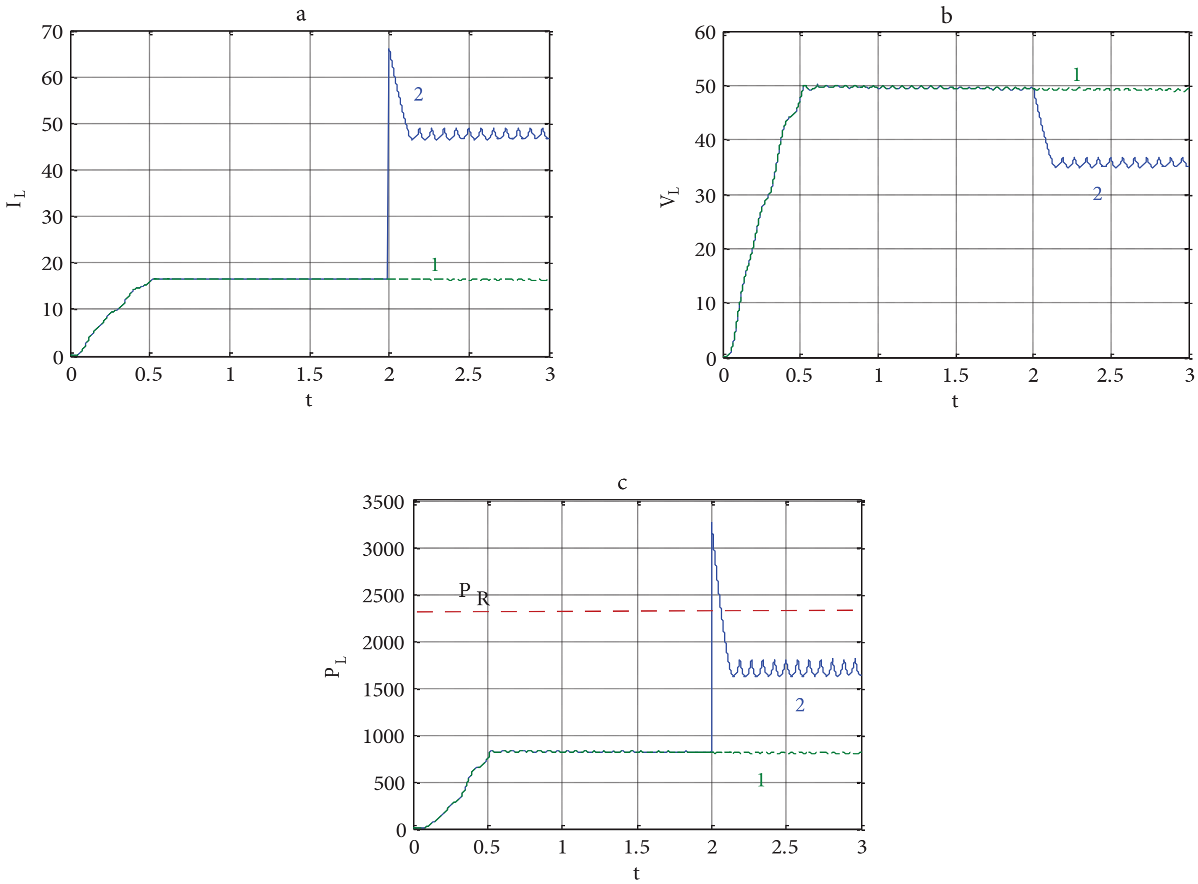

Figure 9. Simulation results showing power regulated DC/DC driver outputs for the right tire motor system (label 1) and the left tire motor system (label 2). The left tire motor system draws high current from the power system due to an isolation fault.

distribution systems. This component is based on two-layer hierarchical control. The bottom layer control provides voltage stability. The top level control limits the power insertion to a desired peak power point. The DC/DC driver component provides online control of DC power distribution.

The proposed power regulated DC/DC driver can be a step towards designing more secure and smart components for DC distribution systems. Implementation of distributed power control strategy by using the DC/DC driver nodes, spread over the power distribution network, facilitates active management of power distribution systems. Fault tolerance and system reliability should be considered as the most important assets for electric vehicle technology because even minor faults may cause severe problems. In this manner, we illustrate an active power management example for electric vehicles by using DC distribution implemented by DC/DC driver nodes.

The simulation results reveal that the proposed maximum power point management can considerably enhance security of power distribution for electric vehicles. However, this approach can also be applied for smart grid applications. Active power management strategies make DC power distribution more secure and smart for future grids.

The findings of this study are based on numerical simulation results. Experimental tests for more realistic

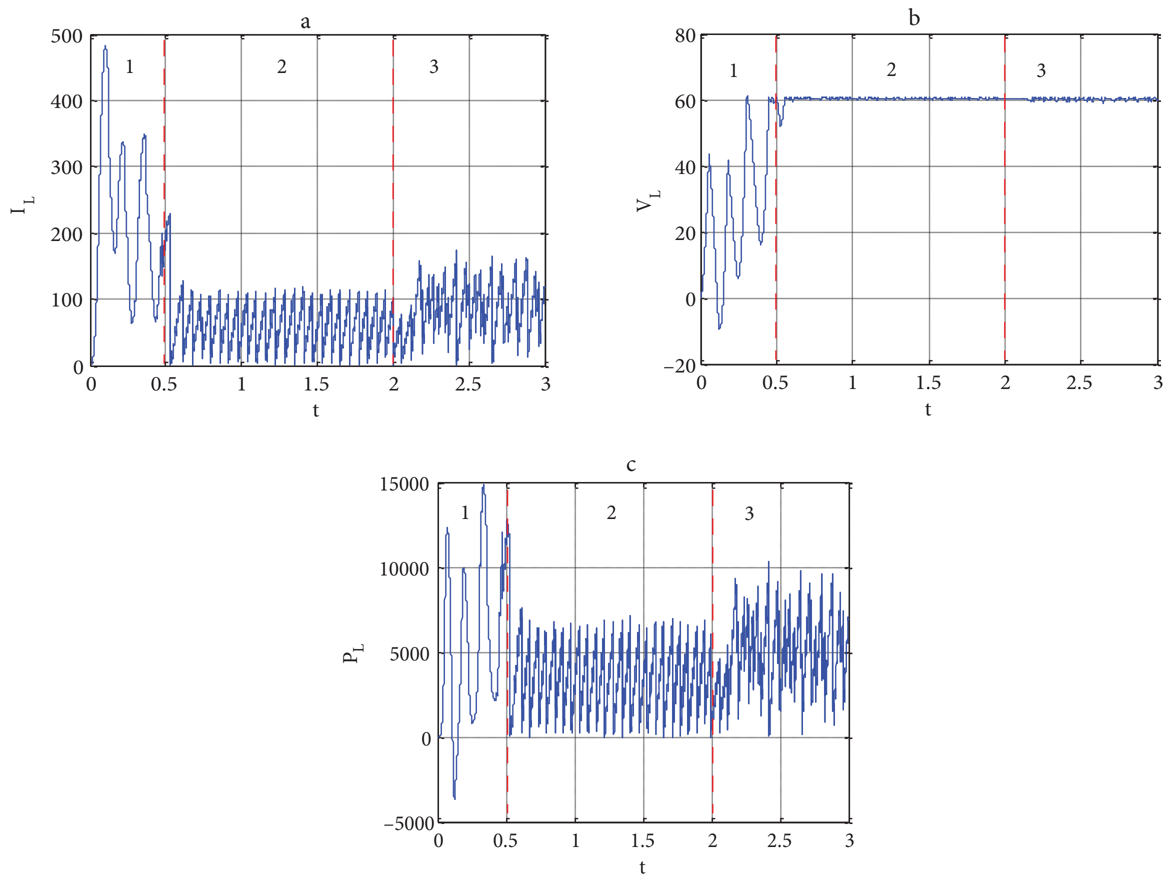

Figure 10. Simulation results showing the output of central power regulated DC/DC driver output supplying the 60 V DC bus. The left tire motor system draws high current from the power system due to an isolation fault at the interval indicated by label 3.

and extreme conditions are necessary for the validation of our theoretical findings. A future study should be devoted to experimental investigation of the system.

References

[1] Hingorani N. High-voltage DC transmission: a power electronics workhorse. IEEE Spectrum 1996; 33: 63–72.

[2] Chaves M, Margato E, Silva FJ, Pinto SF, Santana J. HVDC transmission systems: bipolar back-to-back diode clamped multilevel converter with fast optimum-predictive control and capacitor balancing strategy. Electr Pow Syst Res 2011; 81: 1436–1445.

[3] Cetin E, Yilanci A, Ozturk HK, Colak M, Kasikci I, Iplikci S. A micro-DC power distribution system for a residential application energized by photovoltaic-wind/fuel cell hybrid energy systems. Energ Buildings 2010; 42: 1344–1352.

[4] Kakigano H, Nomura M, Ise T. Loss evaluation of DC distribution for residential houses compared with AC system. In: International Power Electronics Conference; 21–24 June 2010; Sapporo, Japan. New York, NY, USA: IEEE. pp. 480–486.

[5] Li W, Mou X, Zhou Y, Marnay C. On voltage standards for DC home microgrids energized by distributed sources. In: IEEE 7th International Power Electronics and Motion Control Conference; 2–5 June 2012; Harbin, China. New York, NY, USA: IEEE. pp. 2282–2286.

[6] Limpaecher R. Novel converters for electric ship propulsion system and shipboard power distribution. In: 24th Power Modulator Symposium; 26–29 June 2000; Norfolk, VA, USA. New York, NY, USA: IEEE. pp. 89–96.

[7] Dale SJ. Ship power system testing and simulation. In: Electric Ship Technologies Symposium; 27 July 2005; Philadelphia, PA, USA. New York, NY, USA: IEEE. pp. 202–205.

[8] Song B, McDowell R, Bushnell A. A three-level DC-DC converter with wide-input voltage operations for ship electric power distribution systems. IEEE T Plasma Sci 2004; 32: 1856–1863.

[9] Chan C. An overview of electric vehicle technology. P IEEE 1993; 81: 1202–1213.

[10] Clement-Nyns K, Haesen E, Driesen J. The impact of vehicle-to-grid on the distribution grid. Electr Pow Syst Res 2011; 81: 185–192.

[11] Karabiber A, Keles C, Kaygusuz A, Alagoz BB. An approach for the integration of renewable distributed generation in hybrid DC/AC microgrid. Renew Energ 2013; 52: 251–259.

[12] Kaygusuz A, Keles C, Alagoz BB, Karabiber A. Renewable energy integration for smart sites. Energ Buildings 2013; 64: 456–462.

[13] Amin M, Arafat Y, Lundberg S, Mangold S. Low voltage DC distribution system compared with 230 V AC. In: IEEE Electrical Power and Energy Conference; 3–5 October 2011; Winnipeg, Canada. New York, NY, USA: IEEE. pp. 340–345.

[14] Geng J, Jin R, Fan Y, Liu B, Li J, Cheng Y, Wang Z. The study on electromagnetic compatibility of DC electric motor in HAPS. Aerosp Sci Technol 2005; 9: 617–625.

[15] Kabalci E, Kabalci Y, Develi I. Modelling and analysis of a power line communication system with QPSK modem for renewable smart grids. Int J Elec Power 2012; 34: 19–28.

[16] Makram EB, Varadan S. Analysis of reactive power and power factor correction in the presence of harmonics and distortion. Electr Pow Syst Res 1993; 26: 211–218.

[17] Bakos GC, Tsagas NF. Technoeconomic assessment of a hybrid solar/wind installation for electrical energy saving. Energ Buildings 2003; 35: 139–145.

[18] Toledo OM, Filho DO, Diniz ASAC. Distributed photovoltaic generation and energy storage systems: a review. Renew Sust Energ Rev 2010; 14: 506–511.

[19] Costa V, dos Santos PM, Borges B. A design methodology for integrated inductor-based DC–DC converters. Microelectr J 2012; 43: 401–409.

[20] Hedlund M. Design and construction of a bidirectional DC-DC converter for an EV application. Uppsala, Sweden: Uppsala University UPTEC F10 013.

[21] Shagar BM, Vinod S, Lakshmi S. Design of DC-DC converter for hybrid wind solar energy system. In: International Conference on Computing, Electronics and Electrical Technologies; 21–22 March 2012; Kumaracoil, India. New York, NY, USA: IEEE. pp. 429–435.

[22] Saha SS. Efficient soft-switched boost converter for fuel cell applications. Int J Hydrogen Energ 2011; 36: 1710–1719.

[23] Liu H, Elmes J, Zhang K, Wu TX, Batarseh I. Low voltage flyback DC-DC converter for power supply applications. In: Proceedings of the IEEE National Aerospace and Electronics Conference (NAECON); 20–22 July 2011; Dayton, OH, USA. New York, NY, USA: IEEE. pp. 215–218.

[24] Mboup AB, Ndiaye PA, Guerin F, Lefebvre D. Control design for hybrid electrical energy systems based on dc/dc converters duty cycle value. In: EVRE Ecological Vehicles Renewable Energies Conference; 2009; Monaco. pp. 1–7.

[25] Valenciaga F, Puleston PF. Supervisor control for a stand-alone hybrid generation system using wind and photovoltaic energy. IEEE T Energy Conver 2005; 20: 398–405.

[26] Keles C, Alagoz BB, Akcin M, Kaygusuz A, Karabiber A. A photovoltaic system model for Matlab/Simulink simulations. In: Fourth International Conference on Power Engineering, Energy and Electrical Drives (POWERENG); 13–17 May 2013; İstanbul, Turkey. New York, NY, USA: IEEE. pp. 1643–1647.

[27] Chung HSH, Chow WC. Development of switched-capacitor-based DC/DC converter with bi-directional power flow. In: Proceedings of the IEEE International Symposium on Circuits and Systems; 30 May–2 June 1999; Orlando, FL, USA. New York, NY, USA: IEEE. pp. 202–205.

[28] Ioinovici A. Switched-capacitor power electronics circuits. IEEE Circuits Syst Mag 2001; 1: 37–42.

[29] Chen W, Round S, Duke R. Design of an auxiliary power distribution network for an electric vehicle. In: International Workshop on Electronic Design, Test & Applications; 29–31 January 2002; Christchurch, New Zealand. New York, NY, USA: IEEE. pp. 257–261.

[30] Stuart T, Fang F, Wang X, Ashtiani C, Pesaran A. A Modular Battery Management System for HEVs. Golden, CO, USA: DOE Office of Advanced Transportation Technologies, National Renewable Energy Laboratory, and Daimler Chrysler, 2002.